



OPEN Quantitative study on objective indicators for assessing motion sickness susceptibility based on Vestibulo-Ocular Reflex experiments

Yue Li^{1,4}, Liwen Pan^{2,4}, Muchen Liu¹, Zhimeng Shao¹, Menghan Xue¹, Jiawei Liao¹, Huanyu Zhao¹, Mingnan Wu², Shen Yu³✉ & Xiang Wu¹✉

Motion sickness (MS) is a common physiological response that often occurs when individuals are exposed to environments with repeated acceleration stimuli. MS results from a mismatch between the vestibular system and visual and proprioceptive inputs. As a crucial organ for sensing acceleration stimuli, the vestibular system is closely related to the onset of MS. However, the complex pathogenesis of MS has led to its diagnosis primarily relying on subjective questionnaires, with a lack of objective indicators for evaluation. To identify objective indicators for evaluating MS, we conducted rotating chair stop experiments based on the principle of vestibulo-ocular reflex with 65 volunteers, obtaining their nystagmus slow-phase velocity and related time constants. Additionally, we conducted detailed MS questionnaires with these volunteers to assess their MS susceptibility. Through correlation analysis, we explored whether the nystagmus slow-phase velocity and related time constants significantly correlated with the MS questionnaire scores. The results showed significant positive correlations between the maximal nystagmus slow-phase velocity, cupula time constant, velocity storage time constant, and the nystagmus duration with the MS questionnaire scores in the 65 volunteers. These results indicated that these nystagmus parameters could serve as objective indicators for assessing MS susceptibility. Using K-Means clustering analysis, we classified MS susceptibility into categories I, II, III, and IV, and conducted K-Means clustering analysis on the corresponding nystagmus slow-phase velocity, cupula time constant, velocity storage time constant, and nystagmus duration. The magnitude and range of these indicators at different levels was quantified, offering objective and quantitative indicators for the clinical diagnosis of MS.

Keywords Motion sickness susceptibility, Nystagmus slow-phase velocity, Cupula time constant, Velocity storage time constant, K-Means clustering analysis

Motion sickness (MS) is a well-documented phenomenon in healthy individuals. The physical manifestations of MS frequently occur during travel by automobile, sea, and airplane, as well as when immersed in virtual reality^{1,2}. The primary symptoms of MS include autonomic reactions such as dizziness, nausea, vomiting, sweating, hypersalivation, pallor, and stomach awareness³. Additionally, languorous syndrome, characterized by persistent fatigue, drowsiness, and lethargy, is also a significant symptom. MS affects nearly one-third of all travelers⁴. Moreover, 40% of pilots experience MS while navigating aircraft. Even more strikingly, up to 90% of sailors suffer from MS during severe weather conditions. MS not only causes significant discomfort but also extends the training cycles for aviation and maritime personnel, impairs job performance, and adversely impacts overall health⁵⁻⁷.

Currently, several hypotheses explained the pathogenesis of MS, with the sensory conflict and neural mismatch hypothesis proposed by Reason and Brand being widely accepted⁸. According to this hypothesis,

¹School of Medical Imaging, Xuzhou Medical University, Xuzhou 221004, China. ²The First Clinical Medical College, Xuzhou Medical University, Xuzhou 221004, China. ³State Key Laboratory of Structural Analysis for Industrial Equipment, Dalian University of Technology, Dalian 116024, China. ⁴Yue Li and Liwen Pan contributed equally. ✉email: yushen@dlut.edu.cn; x_wu@xzhmu.edu.cn

MS occurred when the input from the visual, vestibular, and proprioceptive systems conflicted with the central nervous system's expected or stored experiential information in an abnormal motion environment⁹. The physiological significance of sensory conflict and neural mismatch lied in promoting the perception of sensory organs of motion information, facilitating continuous self-learning and adjustment, and ultimately forming an adaptation to abnormal motion¹⁰. Generally, most individuals experience MS due to repeated acceleration stimuli¹¹. The vestibular system, responsible for sensing acceleration stimuli, is closely related to the onset of MS. Some studies indicated that subjects without vestibular labyrinth function did not develop MS¹², and even those with impaired vestibular labyrinth function exhibited some immunity to MS¹³. Therefore, a normally functioning vestibular system in the inner ear is necessary for the development of MS. Due to the unclear and complex mechanisms of MS, its evaluation standards primarily relied on subjective questionnaires^{14–16}. However, these methods remained susceptible to subjective bias, and the responses provided by subjects might introduce occasional errors during the survey.

The vestibular system, functioning as the body's balance organ, is essential for perceiving acceleration stimuli and maintaining equilibrium¹⁷. When stimulated by acceleration, vestibular receptors convert physical stimuli into electrical signals, which are then transmitted to the brain. This process induces involuntary nystagmus, a phenomenon known as the vestibulo-ocular reflex (VOR) mechanism¹⁸. For individuals with normal vestibular function, we hypothesized that the semicircular canals and otolithic organs share certain vestibular characteristics related to MS susceptibility. While the semicircular canals detect angular acceleration and the otolithic organs are primarily sensitive to linear acceleration, both contribute to the vestibular system's role in balance and spatial perception. We proposed that the vestibular system's inherent sensitivity is not confined to angular acceleration stimuli but may also influence an individual's response to linear acceleration experienced during daily transportation. By studying parameters associated with the semicircular canals, we expected to capture these intrinsic properties of the vestibular system, which may be linked to MS susceptibility under different types of acceleration. This study focused on four key parameters: the cupula time constant, velocity storage time constant, nystagmus slow-phase velocity (SPV), and nystagmus duration. The cupula time constant is an intrinsic parameter of the vestibular system, reflecting the response time of the cupula receptors and indicating the speed at which the vestibular system perceives and restores balance. The velocity storage time constant represents the duration for which vestibular signals are stored and prolonged in the brainstem. The nystagmus SPV serves as an objective measure of the vestibular system's response to acceleration¹⁹. Nystagmus duration reflects the sustained response of the vestibular system to angular acceleration, encompassing the combined effects of the cupula time constant and the velocity storage time constant. These parameters may be related to an individual's MS susceptibility. To identify the objective indicators for evaluating MS, we conducted VOR experiments to obtain the nystagmus SPV, cupula time constant, velocity storage time constant, and nystagmus duration from volunteers, alongside MS questionnaires to assess MS susceptibility. Correlation analysis was used to examine the relationship between these parameters and MS susceptibility. Objective indicators meeting the criteria were further analyzed using K-Means clustering.

Results

Nystagmus characteristics

All 65 volunteers exhibited horizontal nystagmus following the sudden stop experiment. For instance, the nystagmus trajectory of one volunteer is shown in Fig. 1. The positive slope segments represent the slow-phase of the nystagmus, while the negative slope segments indicate the fast-phase of the nystagmus. Interrupted segments of the trajectory curves denote instances of eye blinking. The absolute value of the trajectory slope represents the velocity of eye movement during both the slow and fast phases of nystagmus. We calculated the average angular velocity of all eye movements in the slow-phase for each second and used this as the SPV for that second. The blue curve in Fig. 2 illustrates the transient changes in the SPV over time for one volunteer. At the initial stage of the sudden stop, the SPV was at its maximum. As time increased, the SPV gradually decreased to zero.

To estimate the cupula time constant and the velocity storage time constant, a step rotational stimulus was applied. The orange curve in Fig. 2 represents the changes in SPV due to the cupula response during the sudden stop. At the initial stage of the sudden stop, the cupula response caused the SPV to reach its peak, which then gradually decreased to zero. The yellow curve in Fig. 2 represents the changes in SPV due to the velocity storage mechanism during the sudden stop. The volunteers' SPV caused by the velocity storage mechanism initially increased and then gradually decreased to 0 over time. We obtained the nystagmus duration, the cupula time constant, the velocity storage time constant, and the maximal SPV for all 65 volunteers (see Fig. 3). The cupula time constants ranged from 1.3 to 20.28 s, with most volunteers having values between 2.44 and 10.71 s. The average cupula time constant was 6.59 ± 4.84 s. The velocity storage time constants ranged from 0.82 to 33.25 s, with most volunteers having values between 10.73 and 18.69 s. The average velocity storage time constant was 15.24 ± 6.76 s. Regarding the nystagmus duration, the 65 volunteers ranging from 19 to 45 s, with most durations falling between 28 and 35 s. The average duration of nystagmus was 31.74 ± 5.99 s. The maximal SPV ranged from 13.79 °/s to 76.38 °/s, with most values between 33.52 °/s and 57.71 °/s. The average maximal SPV was 41.73 ± 14.88 °/s.

Correlation analysis

The scores from the three MS questionnaires administered to the 65 volunteers are presented in Fig. 4. We conducted a correlation analysis on these scores. The results indicated a significant correlation among the scores of the three MS questionnaires ($P < 0.01$). Detailed correlation analysis table was provided in the supplementary materials. Given that the MSAQ encompassed a more comprehensive range of MS indicators, we performed a correlation analysis between the MSAQ scores of the 65 volunteers and their cupula time constants, velocity

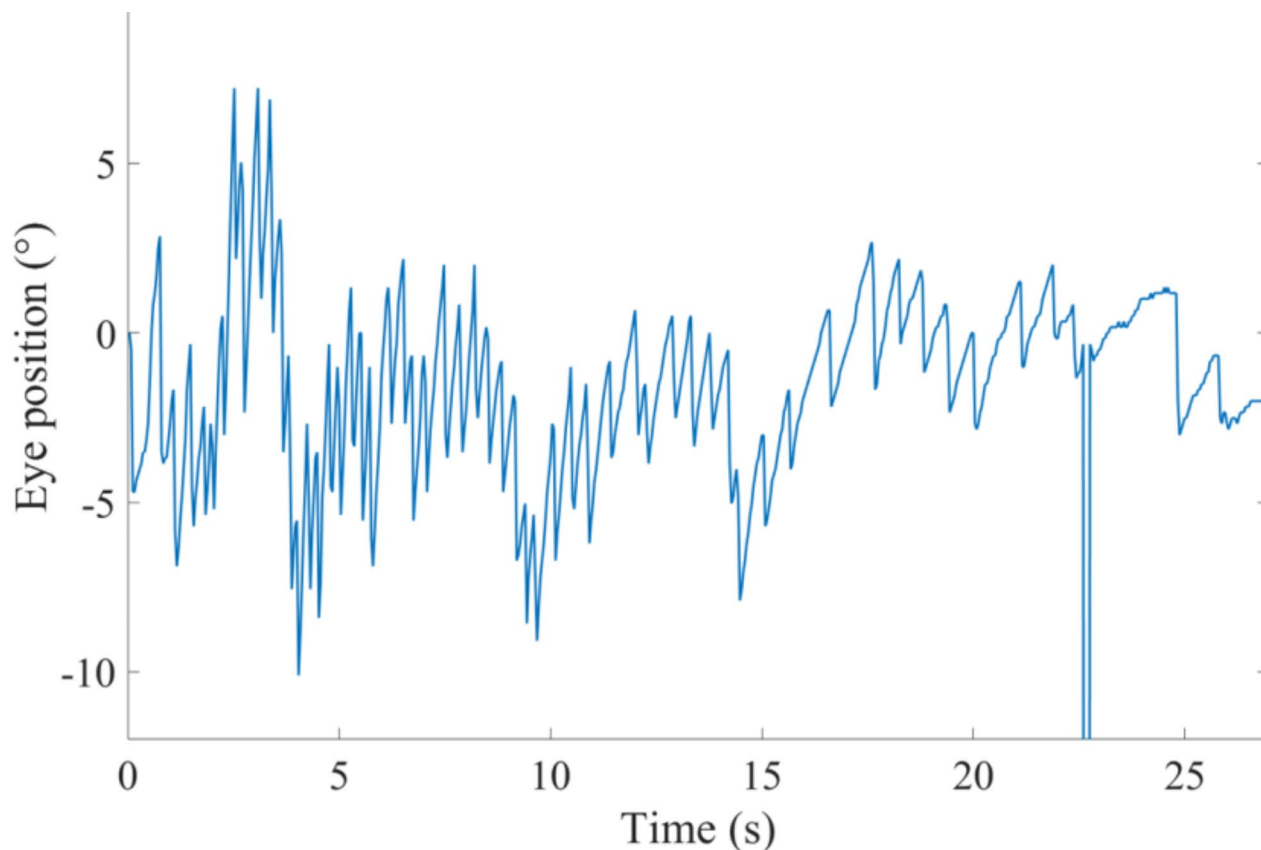


Fig. 1. The trajectory curve of a volunteer's nystagmus.

storage time constants, nystagmus durations, and maximal SPV. As shown in Table 1, the analysis revealed significant correlations between the MSAQ scores and the cupula time constant, velocity storage time constant, nystagmus duration, and maximal SPV ($P < 0.05$). Additionally, the scatter plots of the MSAQ scores from the 65 volunteers and the objective parameters, including the cupula time constant, velocity storage time constant, nystagmus SPV, and nystagmus duration, are shown in Fig. 5A, B and C, and 5D, respectively.

K-means clustering analysis

To perform K-means clustering analysis on the cupula time constant, velocity storage time constants, nystagmus durations, and maximal SPV, which were significantly correlated with the volunteers' MS scores, we first applied the elbow method to determine the optimal number of clusters (K) for the MS questionnaire scores of the 65 volunteers. The rate of decrease in the sum of squared errors (SSE) slowed noticeably after $K = 4$. Therefore, we selected $K = 4$, categorizing the MS susceptibility into four levels: I (none), II (slight), III (moderate), and IV (severe).

As presented in Table 2, the MSAQ scores show significant differences among the clusters ($p < 0.01$). The MSAQ categories I, II, III, and IV correspond to the following mean \pm standard deviation scores (%): I: 22.23 ± 4.83 , II: 37.84 ± 3.35 , III: 47.12 ± 2.68 , and IV: 59.76 ± 3.38 . The centroid values for these categories are 22.23, 37.84, 47.12, and 59.76, respectively. Moreover, we also performed K-means clustering analysis on the SPV, cupula time constants, velocity storage time constants, and nystagmus durations, which were correlated with the MSAQ scores. Corresponding to the MSAQ categories I, II, III, and IV, there are significant differences in SPV, cupula time constants, velocity storage time constants, and nystagmus durations among the clusters ($P < 0.01$), as shown in Table 2. The ranges for SPV, cupula time constants, velocity storage time constants, and nystagmus durations corresponding to the MSAQ categories I, II, III, and IV are detailed in Table 3.

Discussion

When the volunteers' heads were subjected to a clockwise horizontal rotational acceleration stimulus, the semicircular canals followed the angular movement of the head. In the normal head position, all 65 volunteers exhibited horizontal nystagmus, with no significant vertical or torsional nystagmus observed. This was because the horizontal semicircular canals were approximately aligned with the horizontal rotational plane, resulting in the excitation of the left horizontal semicircular canal and inhibition of the right horizontal semicircular canal. Under the influence of the VOR mechanism, this caused horizontal slow-phase eye movements to the right, opposite to the direction of head acceleration, aiding in maintaining visual stability and body balance^{20,21}. The displacement of the cupula within the anterior and posterior semicircular canals was minimal compared

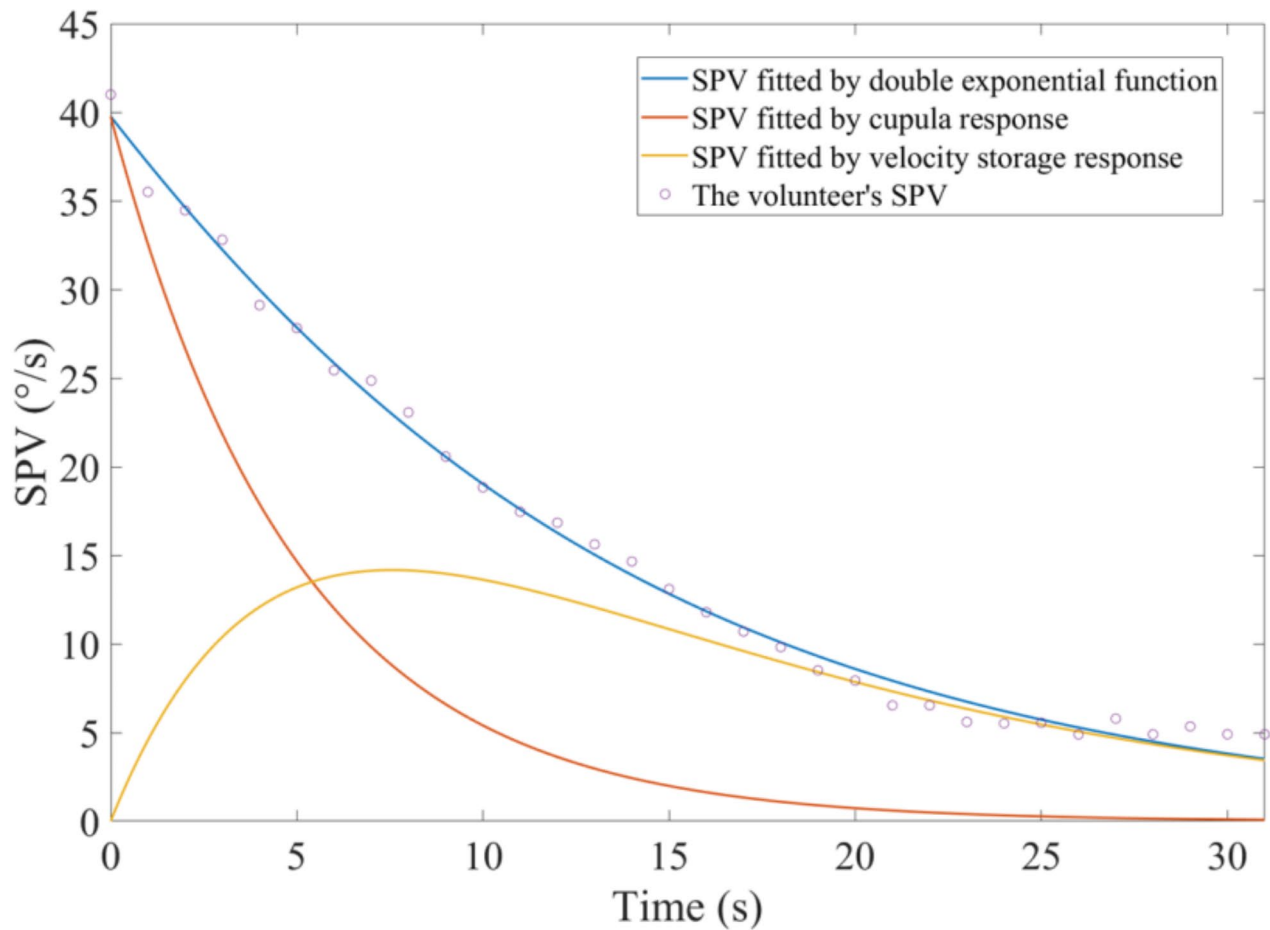


Fig. 2. The trajectory curve of a volunteer's nystagmus SPV in the time domain.

to that in the horizontal semicircular canal because the anterior and posterior semicircular canals were nearly perpendicular to the rotational plane^{17,22}. Consequently, the anterior and posterior semicircular canals did not receive strong stimulation and did not produce significant vertical or torsional nystagmus.

During the sudden stop experiment, a sudden decrease in the velocity of the rotating chair resulted in a momentary large acceleration. This acceleration stimulated the vestibular systems, triggering the VOR mechanism to induce involuntary nystagmus in the volunteers. The volunteers' nystagmus SPV reached its peak instantaneously at the initial moment. After the sudden stop of the rotating chair, the angular acceleration disappeared, and the cupular receptors in the semicircular canals gradually returned to their resting positions due to their inherent elastic restorative force²⁰. As a result, the volunteers' nystagmus SPV decreased from its initial peak to zero (see the blue line in Fig. 2). As shown in Fig. 3, the average maximum SPV for the 65 volunteers was 41.73 ± 14.88 °/s when subjected to the same angular acceleration. There were variations in the maximal nystagmus SPV among different volunteers, reflecting individual differences. Additionally, the MSAQ scores varied among the 65 volunteers, further highlighting individual differences. The significant correlation between the MSAQ scores and the maximal nystagmus SPV suggested that SPV could serve as an objective measure of MS susceptibility, further confirming the close relationship between the vestibular system and MS.

As shown in Table 1, there is a positive correlation between the volunteers' SPV and their MSAQ scores, indicating larger SPV corresponds to higher MS susceptibility. When the head is subjected to angular acceleration, there is a quantitative relationship between the SPV and the deformation of the cupula in the horizontal semicircular canal¹⁹. Under the same rotational conditions, individual differences caused varying degrees of cupula deformation in the volunteers' vestibular semicircular canals. Greater cupula deformation led to larger SPV, which in turn resulted in higher MSAQ scores and increased MS susceptibility. Thus, individuals with a more sensitive vestibular system may exhibit larger cupula responses, greater SPV, and higher MS susceptibility. The variability in vestibular system responses among individuals is a significant factor influencing MS susceptibility.

Additionally, we used the method provided by Dai et al. to measure the SPV and estimate the cupula time constants and velocity storage time constants for the volunteers²³. This method effectively distinguishes between the time constants of neural discharge activity in the direct pathway of the eighth cranial nerve and those in the central velocity storage mechanism. Since the time constant of neural discharge activity in the direct pathway of the eighth cranial nerve depends solely on the mechanical relaxation time constant of the cupula and the

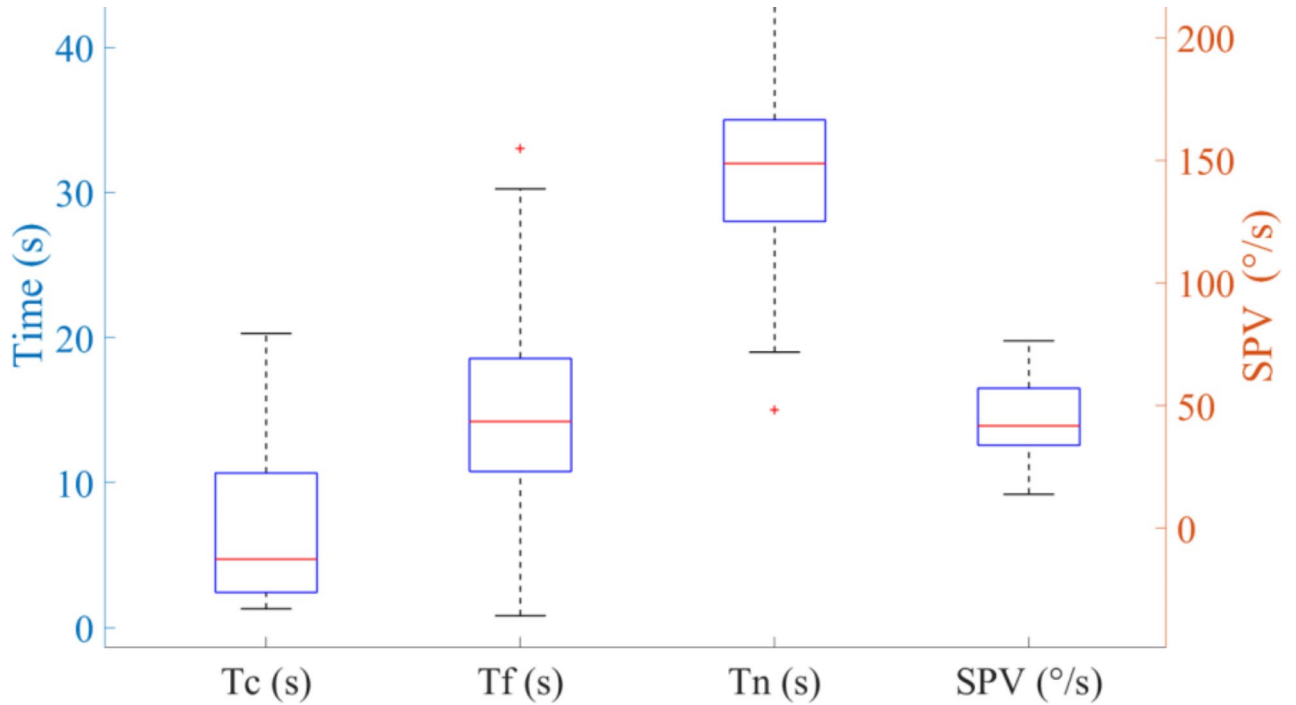


Fig. 3. Box plots of the range of cupula time constants, velocity storage time constants, nystagmus durations, and SPV for 65 volunteers. Tc represents the cupula time constant. Tf represents the velocity storage time constant. Tn represents the nystagmus duration.

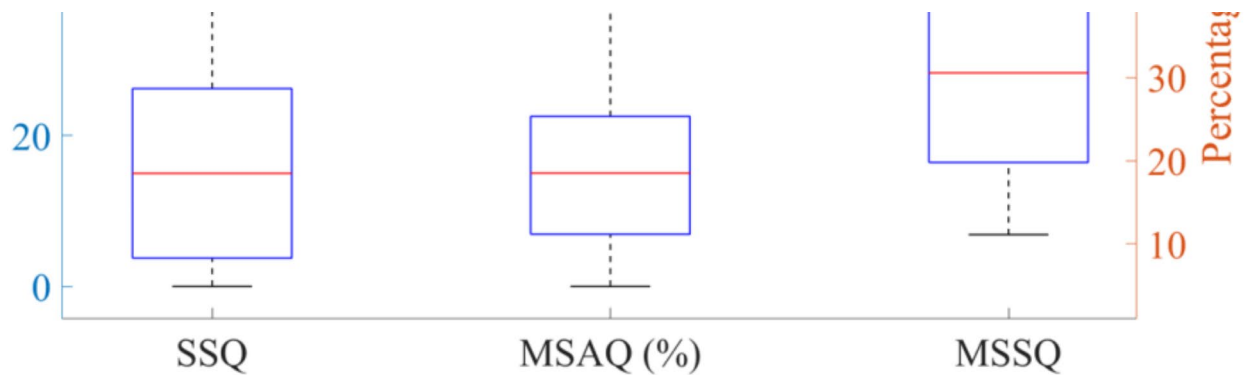


Fig. 4. Box plots of the range of SSQ, MSAQ, and MSSQ scores for 65 volunteers.

Correlation					
Parameters		SPV	Cupula time constant	Velocity storage time constant	Nystagmus duration
MSAQ	Correlation Coefficient	0.32	0.25	0.45	0.84
	Sig. (2-tailed)	$P < 0.01$	$P < 0.05$	$P < 0.01$	$P < 0.01$

Table 1. Correlation analysis between the MSAQ scores and the cupula time constant, velocity storage time constant, nystagmus duration, and maximal SPV for 65 volunteers.

transduction process of hair cells, this method is currently an effective way to estimate the cupula time constant using nystagmus measurements. The cupula time constants of the 65 volunteers ranged from 1.30 to 20.28 s, with an average of 6.59 ± 4.84 s, which is close to the 4.2 s measured by Dai et al., thereby confirming the reliability of our experimental results. Correlation analysis revealed a significant relationship between the cupula time constant and MSAQ scores among the 65 volunteers, indicating that the cupula time constant could be directly used to measure MS susceptibility. Besides, we also measured the velocity storage time constants for the 65

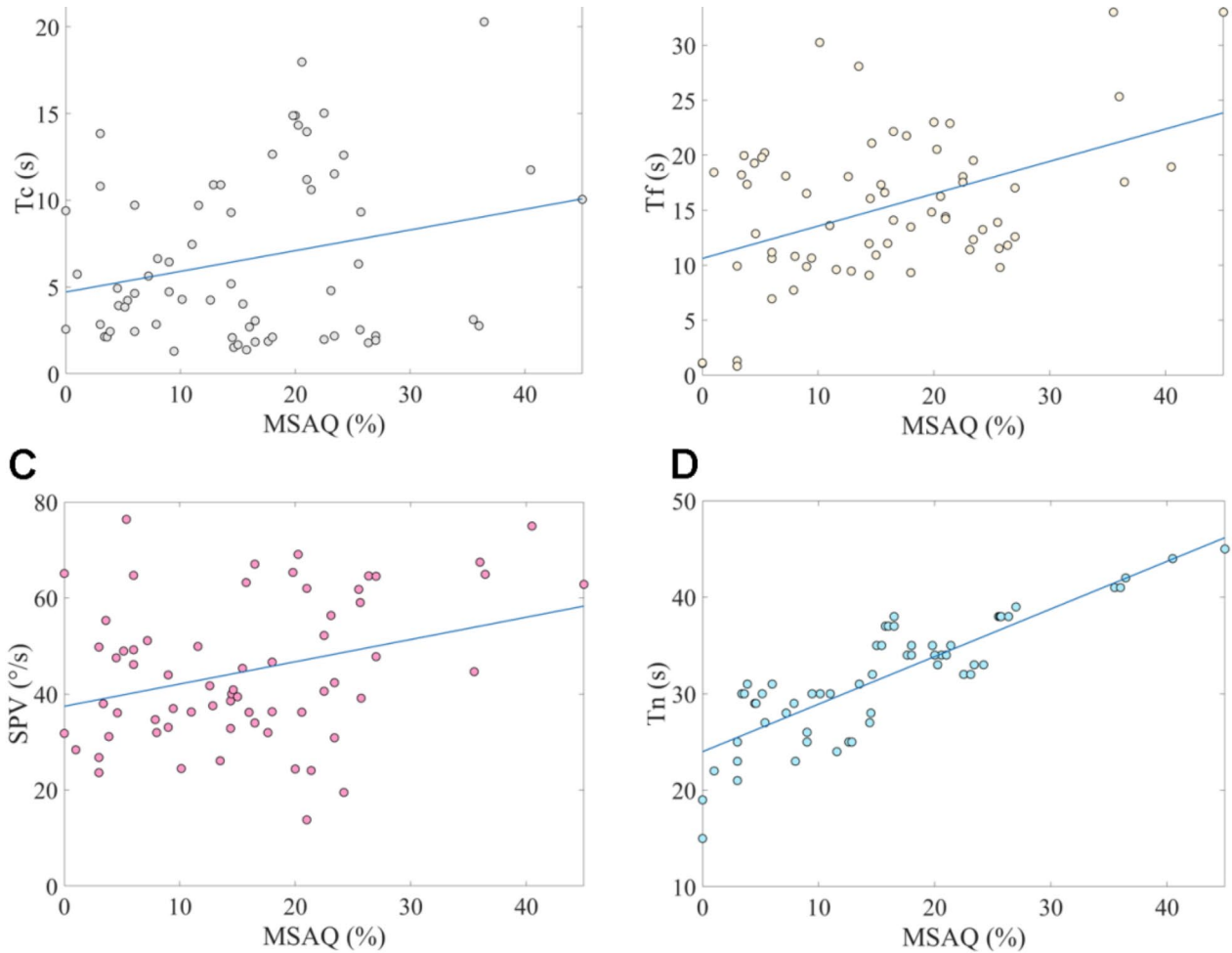


Fig. 5. (A) Scatter plot of MSAQ scores and the cupula time constant from 65 volunteers. Tc represents the cupula time constant. Pearson correlation coefficient = 0.25, $P = 0.04$. (B) Scatter plot of MSAQ scores and the velocity storage time constant from 65 volunteers. Tf represents the velocity storage time constant. Pearson correlation coefficient = 0.45, $P = 2e-4$. (C) Scatter plot of MSAQ scores and the nystagmus SPV from 65 volunteers. Pearson correlation coefficient = 0.32, $P = 9.7e-3$. (D) Scatter plot of MSAQ scores and the nystagmus duration from 65 volunteers. Tn represents the nystagmus duration. Pearson correlation coefficient = 0.84, $P = 1.68e-18$.

Clustering Categories (Mean ± Standard Deviation)						
	Category I	Category II	Category III	Category IV	F	P
MSAQ (%)	22.23 ± 4.83	37.84 ± 3.35	47.12 ± 2.68	59.76 ± 3.38	210.03	<0.01
SPV (°/s)	23.45 ± 4.38	36.34 ± 3.49	48.99 ± 3.64	65.82 ± 4.54		
Cupula time constant (s)	2.22 ± 0.51	5.12 ± 1.08	10.69 ± 1.12	15.64 ± 2.28		
Velocity storage time constant (s)	1.08 ± 0.20	11.40 ± 2.04	18.94 ± 2.04	29.16 ± 3.26		
Nystagmus duration (s)	22.46 ± 3.14	29.25 ± 1.59	33.63 ± 1.12	39.47 ± 2.56		

Table 2. Clustering categories for the MSAQ scores, cupula time constants, velocity storage time constants, nystagmus durations, and maximal SPV for 65 volunteers.

volunteers, which ranged from 0.82 to 33.25 s, with an average of 15.24 ± 6.76 s. Correlation analysis showed a significant relationship between the velocity storage time constant and MSAQ scores for the 65 volunteers, suggesting that the velocity storage time constant could also directly indicate MS susceptibility.

Additionally, we found a significant correlation between the nystagmus duration and MSAQ scores, indicating that the nystagmus duration following the sudden stop experiment could also serve as an indicator

	SPV (°/s)	Cupula time constant (s)	Velocity storage time constant (s)	Nystagmus duration (s)
Category I	(-∞,29.39]	(-∞,3.67]	(-∞,6.24]	(-∞,25.85]
Category II	[29.39,42.66)	[3.67,7.91)	[6.24,15.17)	[25.85,31.44)
Category III	[42.66,114.81)	[7.91,13.17)	[15.17,24.05)	[31.44,36.55)
Category IV	[114.81,+∞)	[13.17,+∞)	[24.05,+∞)	[36.55,+∞)

Table 3. The ranges of SPV, cupula time constants, velocity storage time constants, and nystagmus durations corresponding to the categories I, II, III, and IV.

of MS susceptibility. From Fig. 2, it can be observed that the nystagmus duration following the sudden stop experiment is closely related to both the cupula time constant and the velocity storage time constant. Nystagmus persisted as long as the effects of cupula deformation or velocity storage continue. The results of the correlation analysis indicated that the nystagmus duration, the cupula time constant, and the velocity storage time constant were significantly correlated with MSAQ scores among the volunteers, indicating that these three indicators were key factors influencing MS susceptibility. The positive correlation between the cupula time constant and MSAQ scores revealed that a greater cupula time constant corresponded to higher MS susceptibility. Cupula stiffness is a crucial factor affecting the cupula time constant; the lower the stiffness, the greater the cupula time constant^{18,20}. Under the same angular acceleration stimulus, lower cupula stiffness results in greater deflection displacement of the cupula, leading to larger nystagmus SPV¹⁹. The cupula time constant is an intrinsic parameter of the vestibular system, dependent solely on the geometrical morphology of the semicircular canals, the properties of the endolymph, and the cupula stiffness¹⁸. The variability in cupula time constants among individuals reflected the individual differences in the vestibular system, with those having a more sensitive vestibular system showing higher MS susceptibility. The average cupula time constant for the 65 volunteers was significantly less than the average velocity storage time constant, indicating that the velocity storage time constant was the important factor affecting the nystagmus duration. The significant correlation between nystagmus duration and MSAQ scores further supported the close relationship between the velocity storage effect and the onset of MS. Correlation analysis also revealed that volunteers with larger velocity storage time constants tended to have greater MSAQ scores and higher MS susceptibility.

In recent studies, several objective physiological indicators, such as electrogastronomy, heart rate, electroencephalography, electromyography, galvanic skin response, and electrocardiography, have been identified as measures of MS susceptibility^{24–26}. These objective indicators reflect the physiological signals that accompany the onset of MS. Researchers have used MS questionnaires to confirm the intensity of these physiological signals, including electrogastronomy, heart rate, electroencephalography, electromyography, galvanic skin response, and electrocardiography. In this study, we also employed MS questionnaires to investigate the relationship between MS susceptibility and four parameters: nystagmus SPV, cupula time constant, velocity storage time constant, and nystagmus duration, demonstrating the reliability of our methodology. Compared to the existing literature, the parameters examined in this study are closely linked to the vestibular system, further expanding our understanding of MS susceptibility, particularly in the application of vestibular physiological responses in the diagnosis of MS. Through the use of the rotate-and-stop experiment, we explored the mechanisms underlying the onset of MS and combined this with K-Means clustering analysis to provide a new quantitative basis for the clinical diagnosis of MS. Future research could integrate various physiological assessment methods (such as electrogastronomy, heart rate, electroencephalography, etc.) to perform multidimensional physiological signal analyses, further investigating individual responses to MS in complex acceleration environments.

In this study, we hypothesized that the semicircular canals and otolithic organs share certain vestibular characteristics related to MS susceptibility. We proposed that the inherent sensitivity of the vestibular system is not confined to angular acceleration stimuli but may also influence an individual's response to linear acceleration experienced during daily transportation. When the vestibular system perceives acceleration stimuli, nystagmus SPV reflects the vestibular system's response to angular acceleration. Rotational or turning stimuli in vehicles may reveal vestibular sensitivity through SPV, with higher SPV indicating a reduced ability to adapt to larger accelerations and an increased risk of MS. The cupula time constant represents the response time of the cupula receptors in the vestibular system, indicating the speed at which the vestibular system perceives and restores balance. A larger cupula time constant suggests a slower vestibular response to angular acceleration, which may result in prolonged discomfort after rotational or turning movements. This has significant implications for the persistence of MS symptoms during excessive acceleration-deceleration or abrupt stops and starts while traveling. The velocity storage time constant indicates the duration for which vestibular signals are stored and prolonged in the brainstem. A larger velocity storage time constant implies that the acceleration signals are extended for a longer period, meaning that even after the vehicle has stopped accelerating, the individual may still feel as though they are moving. This prolonged sensation of motion can increase the severity of MS. While traveling, passengers frequently experience excessive acceleration, deceleration, and turning stimuli. The vestibular system continuously perceives and transmits signals during these changes, and the velocity storage mechanism may exacerbate this delayed perception or sensory conflict. The cumulative effect of sensory conflict, particularly when visual, vestibular, and proprioceptive inputs are inconsistent, can gradually intensify MS symptoms. We investigated these parameters through VOR experiments. The significant correlation between these parameters and MSAQ scores suggests that they may be useful for evaluating MS susceptibility. However, this study has certain limitations, as the repeated linear accelerations encountered during actual transportation are highly complex, and these complexities may not be fully captured by parameters such as the cupula time

constant, nystagmus SPV, velocity storage time constant, and nystagmus duration. To further investigate the hypothesis that individuals' MS susceptibility may possess a unique sensitivity to repeated acceleration stimuli, future research should explore the effects of multiple rotate-and-stop stimuli or different types of acceleration stimuli on these parameters.

Conclusions

In this study, we identified that the maximal nystagmus SPV, the cupula time constant, the velocity storage time constant, and the nystagmus duration could serve as objective indicators of MS susceptibility. Furthermore, we employed K-means clustering analysis to categorize MS susceptibility into four levels: I (none), II (slight), III (moderate), and IV (severe). Corresponding nystagmus SPV, cupula time constant, velocity storage time constant, and nystagmus duration were also analyzed using K-means clustering. The magnitudes and ranges of nystagmus SPV, cupula time constant, velocity storage time constant, and nystagmus duration for different levels of MS susceptibility were quantified, providing an objective and quantitative basis for the clinical diagnosis of MS.

Materials and methods

Volunteers

Sixty-five healthy volunteers, with a gender ratio close to 1:1 and aged between 18 and 22 years, voluntarily participated in the experiment after providing written consent. They were thoroughly informed about the experimental procedures and assured that the experiment would involve no risks. Additionally, all volunteers were confirmed to be free of any obvious vestibular disorders and in normal health, as a non-functional vestibular system is immune to MS^{27,28}. Participants were also allowed to withdraw from the experiment at any time without providing a reason, and they consented to the publication of their experimental images. This study was approved by the Ethics Committee for Biology and Medicine at Dalian University of Technology (registration number 2020-077), and all experimental procedures complied with the principles of the Declaration of Helsinki.

MS questionnaire survey

The classic questionnaire was proposed by Reason and Brand; however, the numerous scoring items result in low acceptance and completion rates among subjects¹⁵. Other questionnaires, such as the MS susceptibility questionnaires (MSSQ), the MS assessment questionnaire (MSAQ), the simulator sickness questionnaire (SSQ), and the Graybiel scoring methods, also included detailed subjective evaluation criteria¹⁶. To ensure that the results of the MS questionnaire survey accurately reflected the volunteers' MS susceptibility, we selected three mainstream MS questionnaires and administered them to 65 volunteers individually^{29–31}. Detailed information about these three questionnaires was provided in the supplementary materials. Besides, the 65 volunteers completed the MSAQ primarily based on their experiences with various modes of transportation in daily life, with a particular emphasis on cars and buses. Therefore, the MSAQ scores reflect the symptoms of MS encountered by the participants in real-world transportation settings. Before the start of the experiment, all 65 volunteers completed the three questionnaires. We then scored the volunteers according to the standards of each questionnaire, obtaining and recording their scores. To validate the effectiveness of the questionnaires in assessing MS susceptibility, we performed a correlation analysis of the scores from the three questionnaires. If the scores were correlated, it would indicate the validity of the questionnaire results. We chose the MSAQ as the primary subjective measure of MS susceptibility due to its comprehensive and detailed evaluation. If the scores from the three questionnaires were not correlated, the questionnaire results were considered invalid data.

VOR experiments

Sixty-five volunteers willingly participated in the VOR experiment. They were informed about the entire experimental procedure and were allowed to terminate the experiment at any time. As shown in Fig. 6A, a volunteer wearing an eye mask sat on a rotatable chair. A small infrared camera was fixed to the left side of the eye mask to record the movements of the left eye. The camera had a frame rate of 50 frames per second. Additionally, a gyroscope was fixed to the right side of the eye mask to measure the instantaneous rotational velocity of the head in real-time, with a sampling frequency of up to 200 Hz; we used a sampling frequency of 50 Hz in this study. The eye mask was securely fastened to the volunteer's head to ensure no relative motion between the mask and the head during rotation. Volunteers wore a safety belt, held the chair's armrests, and used a headrest and backrest to increase physical restraint and minimize head movement during the rotation.

Before the experiment began, volunteers sat on the rotatable chair and fastened the safety belt. They then donned the eye mask, and the position of the eye mask was adjusted to allow the infrared camera to record the movements of the left eye accurately. The experiment began with the heads of volunteers in the normal position, facing forward, as shown in Fig. 6B. To obtain nystagmus characteristics and calculate the nystagmus time constants, we used a sudden stop test. The rotatable chair accelerated from 0 to 30 r/min and then maintained a constant clockwise horizontal rotation. Once the volunteer exhibited no significant nystagmus, the chair's brake system was activated to abruptly reduce the rotation speed to 0, achieving a sudden stop. During the sudden stop, the volunteer exhibited eye movements that gradually diminished. These eye movements were recorded and saved for subsequent processing to obtain nystagmus characteristics. All experiments were conducted in a dark room to eliminate light interference with eye movements. If a volunteer needed to undergo multiple experiments, they rested for at least 30 min between sessions to avoid adaptation and significant experimental error due to repeated short-interval testing.

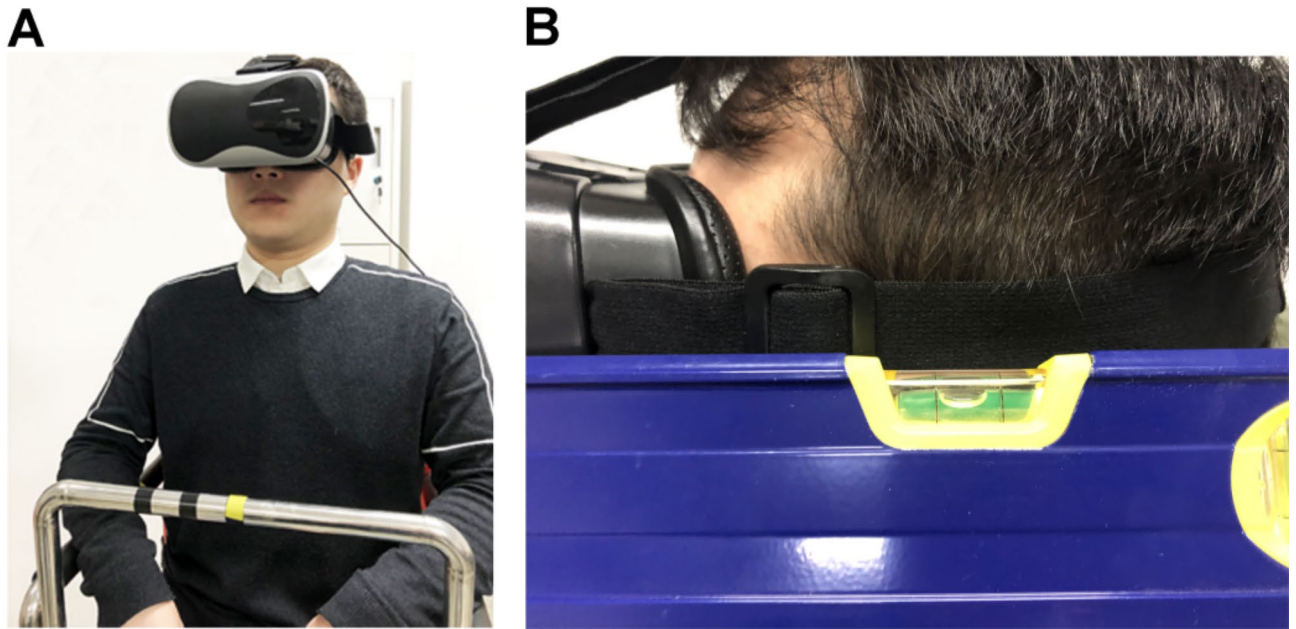


Fig. 6. (A) A volunteer sitting on the rotatable chair. (B) A volunteer's head maintains a normal head position.

Data processing and analysis

We used MATLAB R2017b software to process the videos of the eye movements. Using image processing techniques, the pupil center was marked and its position was located (see Fig. 7). For volunteers with normal vestibular function, the eye movements induced by the VOR mechanism in both eyes are generally consistent³²; thus, only the left eye's movements were recorded and processed in this study. Following the method provided in the literature³³, eye movements with a slow-phase duration of less than 50 ms were removed. To reduce statistical error, the first and last data of each slow-phase of nystagmus, as well as data recorded during eye blinks, were excluded. The nystagmus SPV was calculated based on the method by Wu et al.¹⁹. Additionally, the average SPV per second was calculated and used as the SPV of the nystagmus per second.

We performed Kendall's correlation analysis on the experimental data and the MSAQ scores of the 65 volunteers using SPSS 26.0 software. Furthermore, we conducted K-means clustering analysis on the MSAQ scores of the 65 volunteers. Before applying the K-means clustering method, we used the elbow method to process the MSAQ scores to determine the optimal K value. Subsequently, we performed K-means clustering analysis on the experimental data of the 65 volunteers that met the criteria of the correlation analysis.

Time constants

In the VOR experiments, we estimated the cupula time constant and the velocity storage time constant using the method described by Dai et al.²³. The decay process of the nystagmus SPV can be modeled using two exponential functions. The first function represents vestibular nerve activity induced by the deflection discharge of the sensory hair cell cilia within the cupula. This activity, driven by a direct pathway of the eighth cranial nerve, signifies the neural response of the cupula to a step rotational stimulus. Its time constant is entirely dependent on the cupula's dynamics and hair cell transduction. The second function represents afferent neural activity generated by the semicircular canals in the central velocity storage mechanism. Therefore, the nystagmus SPV in volunteers results from the combined responses of the cupula and the central velocity storage mechanism and can be represented by a double exponential function^{23,34,35}:

$$y(t) = V_1 e^{-\frac{t}{T_c}} + \frac{V_2}{\frac{1}{T_f} - \frac{1}{T_c}} \left(e^{-\frac{t}{T_c}} - e^{-\frac{t}{T_f}} \right) \quad (1)$$

where $y(t)$ is the SPV at time t , V_1 is the gain velocity induced by step rotational angular acceleration in the direct vestibular nerve pathway, V_2 is the gain velocity induced in the central velocity storage mechanism, T_c is the cupula time constant, and T_f is the velocity storage time constant. When the volunteer's head begins to experience a step rotational stimulus, the nystagmus SPV starts to decay. By fitting Eq. (1) to the nystagmus SPV curve induced by the step rotational stimulus, we estimated the cupula time constant and the velocity storage time constant for each volunteer.

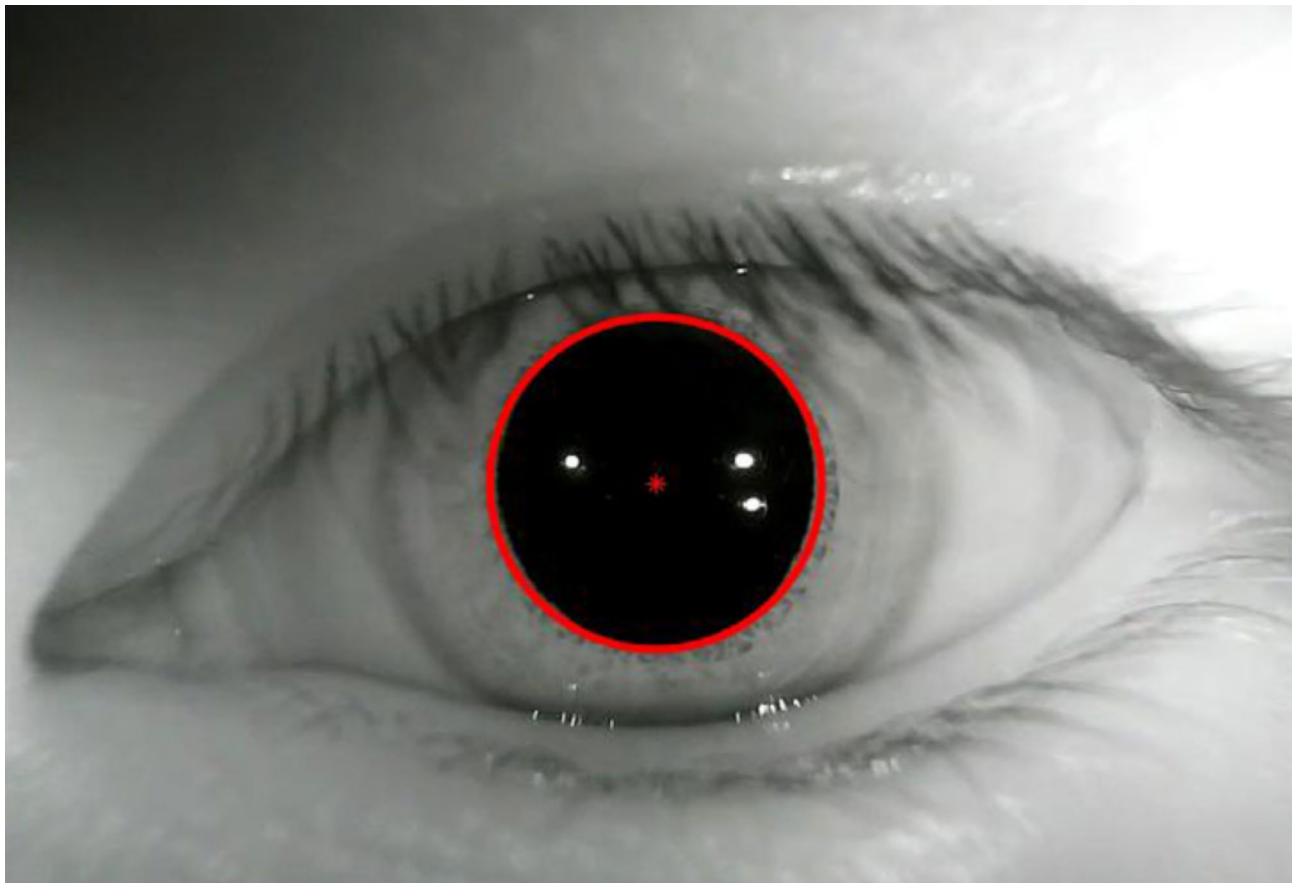


Fig. 7. Pupil location.

Data availability

The original data generated and analysed during the current study and the analysis code are available from the corresponding author upon reasonable request.

Received: 1 July 2024; Accepted: 18 November 2024

Published online: 20 November 2024

References

1. Yeo, S. S., Kwon, J. W. & Park, S. Y. EEG-based analysis of various sensory stimulation effects to reduce visually induced motion sickness in virtual reality. *Sci. Rep.* **12**, 18043 (2022).
2. Molefi, E., McLoughlin, I. & Palaniappan, R. On the potential of transauricular electrical stimulation to reduce visually induced motion sickness. *Sci. Rep.* **13**, 3272 (2023).
3. Lackner, J. R. Motion sickness: more than nausea and vomiting. *Exp. Brain Res.* **232**, 2493–2510 (2014).
4. Rine, R. M., Schubert, M. C. & Balkany, T. J. Visual-vestibular habituation and balance training for motion sickness. *Phys. Ther.* **79**, 949–957 (1999).
5. Van Marion, W. F. et al. Influence of transdermal scopolamine on motion sickness during 7 days' exposure to heavy seas. *Clin. Pharmacol. Ther.* **38**, 301–305 (1985).
6. Jadvar, H. Medical imaging in microgravity. *Aviat. Sp. Environ. Med.* **71**, 640–646 (2000).
7. Landolt, J. P. & Monaco, C. Seasickness in totally-enclosed motor-propelled survival craft: remedial measures. *Aviat. Sp. Environ. Med.* **63**, 219–225 (1992).
8. Reason, J. T. Motion sickness adaptation: a neural mismatch model. *J. R. Soc. Med.* **71**, 819–829 (1978).
9. Tal, D., Wiener, G. & Shupak, A. Mal De Debarquement, motion sickness and the effect of an artificial horizon. *J. Vestib. Res. Equilib. Orientat.* **24**, 17–23 (2014).
10. Oman, C. M. Are evolutionary hypotheses for motion sickness just-so. *Stories? J. Vestib. Res. Equilib. Orientat.* **22**, 117–127 (2012).
11. Shupak, A. & Gordon, C. R. Motion sickness: advances in pathogenesis, prediction, prevention, and treatment. *Aviat. Sp. Environ. Med.* **77**, 1213–1223 (2006).
12. Cheung, B. S., Howard, I. P. & Money, K. E. Visually-induced sickness in normal and bilaterally labyrinthine-defective subjects. *Aviat. Sp. Environ. Med.* **62**, 527–531 (1991).
13. Kennedy, R. S. et al. Symptomatology under storm conditions in the North Atlantic in control subjects and in persons with bilateral labyrinthine defects. *Acta Otolaryngol.* **66**, 533–540 (1968).
14. Cha, Y. H. et al. Motion sickness diagnostic criteria: Consensus document of the classification committee of the Bárány society. *J. Vestib. Res.* **31**, 327–344 (2021).
15. Lamb, S. & Kwok, K. C. S. MSSQ-short norms may underestimate highly susceptible individuals: updating the MSSQ-short norms. *Hum. Factors.* **57**, 622–633 (2015).

16. Cha, Y. H. et al. Mal De Debarquement syndrome diagnostic criteria: Consensus document of the Classification Committee of the Barany Society. *J. Vestib. Res.* **30**, 285–293 (2020).
17. Rabbitt, R. D. et al. Dynamic displacement of normal and detached semicircular canal cupula. *J. Assoc. Res. Otolaryngol.* **10**, 497–509 (2009).
18. Rabbitt, R. D. Semicircular canal biomechanics in health and disease. *J. Neurophysiol.* **121**, 732–755 (2019).
19. Wu, X., Yu, S., Liu, W. & Shen, S. Numerical modeling and verification by nystagmus slow-phase velocity of the function of semicircular canals. *Biomech. Model. Mechanobiol.* **19**, 2343–2356 (2020).
20. Wu, X., Yu, S., Shen, S. & Liu, W. Quantitative analysis of the biomechanical response of semicircular canals and nystagmus under different head positions. *Hear. Res.* **407**, 108282 (2021).
21. Zhang, J. et al. Investigation on biomechanical responses in bilateral semicircular canals and nystagmus in vestibulo-ocular reflex experiments under different forward-leaning angles. *Front. Bioeng. Biotechnol.* **12**, 1322008 (2024).
22. Wu, X., Yu, S., Shen, S. & Liu, W. Exploring the biomechanical responses of human cupula by numerical analysis of temperature experiments. *Sci. Rep.* **11**, 8208 (2021).
23. Dai, M. J., Klein, A., Cohen, B. & Raphan, T. Model-based study of the human cupular time constant. *J. Vestib. Res.* **9**, 293–301 (1999).
24. Gruden, T. et al. Electrogastronomy in autonomous vehicles—an objective method for assessment of motion sickness in simulated driving environments. *Sensors* **21**, 550 (2021).
25. Irmak, T., Pool, D. M. & Happee, R. Objective and subjective responses to motion sickness: the group and the individual. *Exp. Brain Res.* **239**, 515–531 (2021).
26. Recenti, M. et al. Toward predicting motion sickness using virtual reality and a moving platform assessing brain, muscles, and heart signals. *Front. Bioeng. Biotechnol.* **9**, 635661 (2021).
27. Tu, L. et al. Alpha-9 nicotinic acetylcholine receptors mediate hypothermic responses elicited by provocative motion in mice. *Physiol. Behav.* **174**, 114–119 (2017).
28. Huang, Y. D., Xia, S. W., Dai, P. & Han, D. Y. Role of AQP1 in inner ear in motion sickness. *Physiol. Behav.* **104**, 749–753 (2011).
29. Czeisler, M. É. et al. Validation of the motion sickness severity scale: secondary analysis of a randomized, double-blind, placebo-controlled study of a treatment for motion sickness. *Plos One.* **18**, e0280058 (2023).
30. Golding, J. F. Predicting individual differences in motion sickness susceptibility by questionnaire. *Pers. Individ. Differ.* **41**, 237–248 (2006).
31. Kennedy, R. S., Lane, N. E., Berbaum, K. S. & Lilienthal, M. G. Simulator Sickness Questionnaire: an enhanced method for quantifying Simulator sickness. *Int. J. Aviat. Psychol.* **3**, 203–220 (1993).
32. Bockisch, C. J., Khojasteh, E., Straumann, D. & Hegemann, S. C. A. Development of Eye position dependency of slow phase velocity during caloric stimulation. *PLoS One.* **7**, e51409 (2012).
33. Bockisch, C. J., Khojasteh, E. & Straumann, D. Eye position dependency of nystagmus during constant vestibular stimulation. *Exp. Brain Res.* **226**, 175–182 (2013).
34. Raphan, T., Matsuo, V. & Cohen, B. Velocity storage in the vestibulo-ocular reflex arc (VOR). *Exp. Brain Res.* **35**, 229–248 (1979).
35. Cohen, H., Cohen, B., Raphan, T. & Waespe, W. Habituation and adaptation of the vestibuloocular reflex: a model of differential control by the vestibulocerebellum. *Exp. Brain Res.* **90**, 526–537 (1992).

Acknowledgements

This study was funded by the Outstanding Talents Start-up Fund Project of Xuzhou Medical University [Nos. D2021062], Jiangsu Training Program of Innovation and Entrepreneurship for Undergraduates [Nos. 202210313066Y], and the National Natural Science Foundation of China [Nos. 12172082, 11772087].

Author contributions

Conceptualization: M.L.; Methodology: X.W.; Software: Z.S. and M.X.; Validation: J.L.; Formal analysis: H.Z.; Investigation: M.W.; Data curation: M.L.; Writing—original draft preparation: Y.L. and L.P.; Writing—review and editing: S.Y., and X.W.; Visualization: S.Y.; Project administration: X.W. Funding acquisition: X.W.

Declarations

Competing interests

The authors declare no competing interests.

Additional information

Supplementary Information The online version contains supplementary material available at <https://doi.org/10.1038/s41598-024-80233-4>.

Correspondence and requests for materials should be addressed to S.Y. or X.W.

Reprints and permissions information is available at www.nature.com/reprints.

Publisher's note Springer Nature remains neutral with regard to jurisdictional claims in published maps and institutional affiliations.

Open Access This article is licensed under a Creative Commons Attribution-NonCommercial-NoDerivatives 4.0 International License, which permits any non-commercial use, sharing, distribution and reproduction in any medium or format, as long as you give appropriate credit to the original author(s) and the source, provide a link to the Creative Commons licence, and indicate if you modified the licensed material. You do not have permission under this licence to share adapted material derived from this article or parts of it. The images or other third party material in this article are included in the article's Creative Commons licence, unless indicated otherwise in a credit line to the material. If material is not included in the article's Creative Commons licence and your intended use is not permitted by statutory regulation or exceeds the permitted use, you will need to obtain permission directly from the copyright holder. To view a copy of this licence, visit <http://creativecommons.org/licenses/by-nc-nd/4.0/>.